Title: Intracellular metabolic changes of *Clostridium acetobutylicum* and promotion to butanol tolerance during biobutanol fermentation

Author: Yan-Feng Wang Juan Tian Zhi-Hua Ji Mao-Yong Song Hao Li

PII: S1357-2725(16)30205-9
DOI: http://dx.doi.org/doi:10.1016/j.biocel.2016.07.031
Reference: BC 4923

To appear in: *The International Journal of Biochemistry & Cell Biology*

Received date: 3-4-2016
Revised date: 22-7-2016
Accepted date: 27-7-2016

Please cite this article as: Wang, Yan-Feng., Tian, Juan., Ji, Zhi-Hua., Song, Mao-Yong., & Li, Hao., Intracellular metabolic changes of Clostridium acetobutylicum and promotion to butanol tolerance during biobutanol fermentation.*International Journal of Biochemistry and Cell Biology* http://dx.doi.org/10.1016/j.biocel.2016.07.031

Graphical Abstract

GC-MS-based metabolomics approach is effective for elucidating underlying response of *Clostridium acetobutylicum* to butanol stress. PLS-DA revealed a group classification and pairwise discrimination, and 27 metabolites with VIP value greater than 1 were extracted by PLS-DA. The metabolic relevance of these compounds in the response of *C. acetobutylicum* to butanol stress was discussed.

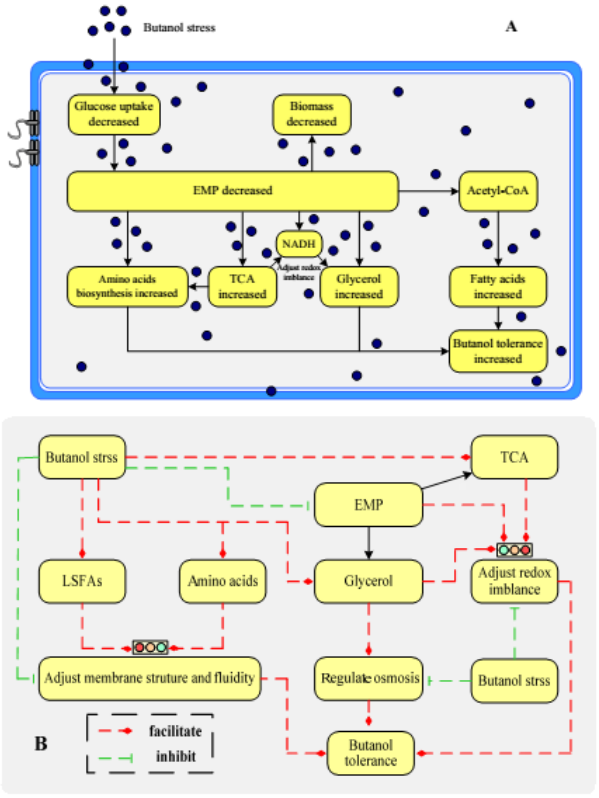

Intracellular metabolic changes of *Clostridium acetobutylicum* and promotion to butanol tolerance during biobutanol fermentation

Yan-Feng Wang [a], Juan Tian [a], Zhi-Hua Ji [a], Mao-Yong Song [b], Hao Li [a,*]

[a] *Beijing Key Laboratory of Bioprocess, College of Life Science and Technology, Beijing University of Chemical Technology, Beijing 100029, China*

[b] *Institute of Environment and Health, Jianghan University, Wuhan 430056, China*

***To whom correspondence should be addressed:**

Hao Li

Beijing Key Laboratory of Bioprocess, College of Life Science and Technology, Beijing University of Chemical Technology, Beijing 100029, P. R. China;

Phone: +86-010-64447747; Fax: +86-010-64416428;

E-mail address: lihao@mail.buct.edu.cn or lihaoh@163.com

Electronic word count: 248 words in the abstract; 4194 words in the main text.

Number of figures: 7; Number of tables: 3.

Financial disclosures: The authors have no financial conflict of interest.

Abbreviations: BCAAs, branched-chain amino acids; DHAP, dihydroxyacetone phosphate; EMP, Embden-Meyerhof-Parnas pathway; GC-MS, gas chromatography-mass spectrometry; HCA,

hierarchical cluster analysis; MSTFA, N-methyl-N-(trimethylsilyl) trifluoroacetamide; PLS-DA, partial least-squares-discriminant analysis; RT-M/Z, retention time-mass to charge ratio; TCA, tricarboxylic acid; TIC, total ion chromatogram; VIP, variable importance in the projection.

ABSTRACT

During the fermentation process, *Clostridium acetobutylicum* cells are often inhibited by the accumulated butanol. However, the mechanism underlying response of *C. acetobutylicum* to butanol stress remains poorly understood. This study was performed to clarify such mechanism through investigating the butanol stress-associated intracellular biochemical changes at acidogenesis phase (i.e., middle exponential phase) and solventogenesis phase (i.e., early stationary phase) by a gas chromatography-mass spectrometry-based metabolomics strategy. With the aid of partial least-squares-discriminant analysis, a pairwise discrimination between control group and butanol-treated groups was revealed, and 27 metabolites with variable importance in the projection value greater than 1 were identified. Under butanol stress, the glycolysis might be inhibited while TCA cycle might be promoted. Moreover, changes of lipids and fatty acids compositions, amino acid metabolism and osmoregulator concentrations might be the key factors involved in *C. acetobutylicum* metabolic response to butanol stress. It was suggested that *C. acetobutylicum* cells might change the levels of long acyl chain saturated fatty acids and branched-chain amino acids to maintain the integrity of cell membrane through adjusting membrane fluidity under butanol stress. The increased level of glycerol was considered to be correlated with osmoregulation and regulating redox balance. In addition, increased levels of some amino acids (i.e., threonine, glycine, alanine, phenylalanine, tyrosine, tryptophan, aspartate and glutamate) might also confer butanol tolerance to *C. acetobutylicum*. These results highlighted our knowledge about the response or adaptation of *C. acetobutylicum* to butanol stress, and would contribute to the construction of feasible butanologenic strains with higher butanol tolerance.

Keywords: *Clostridium acetobutylicum*; Biobutanol; Butanol stress; Metabolomics; Gas chromatography-mass spectrometry.

1. Introduction

Energy crisis and environmental pollution caused by overutilization of traditional fossil fuel promote the demand for alternative novel fuel. As a renewable gasoline substitute, biobutanol is an attractive fuel due to its lower water absorption, higher energy content, and better blending ability; moreover, biobutanol can also be used in conventional combustion engines without any modifications (Dürre, 2007; Zheng et al., 2009).

Biobutanol can be produced by microbial fermentation (Gu et al., 2011), and *Clostridium acetobutylicum*, *C. saccaroperbutylacetonicum*, *C. beijerinckii*, and *C. saccharoacetobutylicum* embrace significant activity for production of biobutanol (Dürre, 2007; Kumar and Gayen, 2011; Green, 2011). Among these solventogenic clostridia, *C. acetobutylicum*, whose genome sequence has been published (Nölling et al., 2001), is the most used microbe for biobutanol production (Dürre, 2007; Lütke-Eversloh and Bahl, 2011). The biobutanol fermentation performed by *C. acetobutylicum* is characterized by acidogenesis phase and solventogenesis phase (Jang et al., 2014). Acidogenesis phase usually occurs during exponential growth, while solventogenesis phase usually occurs at stationary phase and the onset of sporulation as a response of acid accumulation (Amador-Noguez et al., 2011; Alsaker et al., 2010; Liao et al, 2015). During the fermentation process, *C. acetobutylicum* is often stressed by different environmental factors, such as hyperoxia stress (Hillmann et al., 2008), high concentration of substrates and the accumulation of toxic products (acids and solvents) (Tomas et al., 2004; Alsaker et al., 2010). Among these stressors, the toxicity of accumulated butanol is an important obstacle for developing industrial feasible butanologenic strains (Ghiaci et al., 2013). Butanol can inhibit *C. acetobutylicum* cell growth

mainly through disruption of membrane fluidity （Baer et al., 1987), inhibition of glucose uptake, nutrient transport and membrane-bound ATPase activity, partially or completely abolishing the approximately constant transmembrane pH gradient (Tomas et al., 2004), and lowering the intracellular ATP concentration (Tomas et al., 2004; Nicolaou et al., 2010).

To maintain the cell survival, microorganisms including *C. acetobutylicum* have evolved a series of stress responses to external stimuli (Ding et al., 2009). For example, increased levels of saturated fatty acid and longer acyl chain fatty acids at the expense of unsaturated chains and shorter acyl chains might confer butanol tolerance to *C. acetobutylicum* and counteract the increased membrane fluidity secondary to butanol challenge during solventogenesis (Baer et al., 1987; Zhao et al., 2003). Moreover, expressions of some stress response genes (*dnaKJ*, *groES*, *hsp18*, and *hsp90*), solvent formation genes (*adc*, *ctfA/B*, and *bdhA* /*B*), amino acid biosynthesis genes (*CAC0892-CAC0896*), fatty acid biosynthesis opern genes, glycolytic genes and sporulation genes also changed in response to the butanol challenge (Tomas et al., 2004; Alsaker et al., 2010); and overexpression of these genes would likely confer butanol tolerance to *C. acetobutylicum* (Alsaker et al., 2010). Based on these progresses, some efforts have been performed to improve butanol tolerance of *C. acetobutylicum* (Knoshaug and Zhang, 2009). For example, up-regulation of expression of *Spo0A* or *groESL* in *C. acetobutylicum* was performed to enhance butanol tolerance and subsequent solvent yield (Alsaker et al., 2004; Tomas et al., 2003). However, the mechanism underlying the butanol tolerance of *C. acetobutylicum* is very complicate and might involve many genes, mRNAs, proteins, and metabolites (Alsaker et al., 2010; Amador-Noguez et al., 2011). Therefore, though much progress has been made, the exact molecular mechanism still remains poorly understood, and a comprehensive understanding of the mechanism at the

systematic level is needed (Amador-Noguez et al., 2011; Leeet al., 2014).

Metabolomics strategy assesses as many metabolites in a biological system as possible (Lee et al., 2014), and allows us to gain an insight into the biochemical changes followed by external stimulus or a pathological insult (Ku et al., 2010). For example, metabolomics strategy-based discovering of acidogenic-solventogenic transition-associated intracellular metabolite changes facilitated deeper understanding of remodeling of central metabolism in *C. acetobutylicum* during solventogenesis (Amador-Noguez et al., 2011). Many previous studies have proven that gas chromatography-mass spectrometry (GC-MS)-based metabolomics approach can effectively analyze metabolic changes. In our previous studies, GC-MS-based strategy was also used to evaluate biochemical changes in *Saccharomyces cerevisiae* (Cui et al., 2015; Li et al., 2012) or *Blakeslea trispora* (Hu et al., 2013). These previous results showed that GC-MS-based metabolomics strategy can provide us a powerful platform for effectively determining the butanol stress-associated biochemical changes in *C. acetobutylicum*.

In this study, to clarify the mechanism underlying response or adaptation of *C. acetobutylicum* to butanol stress, a GC-MS-based metabolomics approach combined with a multivariate analysis were performed to determine the butanol stress-associated *C. acetobutylicum* intracellular metabolic changes at two distinct fermentation phases (i.e., acidogenic and solventogenic phases).

2. Materials and methods

2.1. Strain, media and culture conditions

C. acetobutylicum ATCC 824 used in this study was purchased from China General Microbiological Culture Collection Center (Beijing, China). Inoculum preparation and batch fermentations were performed in an anaerobic chamber (YQX-Ⅱ, CIMO, China) with an mixed atmosphere containing 90% nitrogen, 5% carbon dioxide and 5% hydrogen (Amador-Noguez et al., 2011).

C. acetobutylicum 824 was cultured anaerobically in PYG medium (5 g/L polypeptone, 5 g/L tryptone, 10 g/L glucose, 10 g/L yeast extract, 8 mg/L $CaCl_2$, 16 mg/L $MgSO_4 \cdot 7H_2O$, 40 mg/L K_2HPO_4, 40 mg/L KH_2PO_4, 0.4 g/L $NaHCO_3$, 0.08 g/L NaCl) at 37°C for 72 h, and subsequently maintained as spores. Inoculant was prepared by heat-activating spores at 80°C for 10 min followed by cooling on ice for 2 min and grown to saturation overnight (Baer et al., 1987).

2.2. Butanol challenge experiments

The precultured *C. acetobutylicum* cells were inoculated into fermentative medium and the initial optical absorbance of 600 nm was adjusted to 0.1. The fermentative culture was performed at 37°C in 250 mL cotton-plugged flasks containing 100 mL of PYG broth either with or without butanol in an anaerobic chamber. For the butanol-treated cells, 0.5%, 1.0%, 1.5%, 2.0%, or 2.5% (v/v) butanol (final concentration) was respectively added into the PYG broth at the beginning of the primary culture.

2.3. Determination of the growth curve

Samples (700 μL) were respectively taken after 0, 1, 2, 4, 8, 12, 16, 20, 24, 28, 32, 36, 40, 48, 60 and 72 h of incubation. *C. acetobutylicum* cell growth curve was determined by measuring the

optical density at 600 nm with a 752 visible spectrophotometer (Shanghai Optical Instrument Factory, Shanghai, China). The experiment was conducted in triplicate.

2.4. Preparation of metabolome samples

It is shown that atmospheric metabolite sampling and processing resulted in quality and quantity of the metabolomics data similar to those obtained using anaerobic processing and pure methanol as the optimal extraction solvent for *C. acetobutylicum* (Lee et al., 2014). In this study, metabolome samples of *C. acetobutylicum* were prepared as previously described (Li et al., 2012) with some modifications. Six biological replicates were performed for each group. Two milliliters of cultures were quickly harvested from middle exponential phase (i.e., the acidogenic phase samples taken after 8 h of cultivation) and early stationary phase (i.e., the solventogenic phase samples taken after 24 h of cultivation) and immediately transferred to 15 mL-tubes containing 8 mL of -40°C pre-chilled methanol-water (60:40, v/v) to quench the intracellular metabolism. Then the cells were collected by centrifugation (5000 g, -4°C, 5 min). The supernatant was discarded, and the pellet was washed by 1 mL of pre-chilled 60% methanol (-40°C). Then the pellet spiked with 50 μL of internal standard (0.5 mg/mL of ribitol in water) was prepared for extraction of intracellular metabolites. The pellet was suspended in 0.75 mL of pre-chilled pure methanol (-40°C) and the mixture was vortexed for 15 s. The suspension was frozen in liquid nitrogen for 5 min and then thawed in an ice bath for 3 min. The freeze-thaw process was repeated three times prior to centrifugation (8000 g, -4°C, 10 min). The supernatant was collected and an additional 0.75 mL of pre-chilled pure methanol was added to the pellet. The mixture was vortexed for 15 s before centrifugation (8000 g, -4°C, 10 min). Both supernatants were pooled together and stored at

-20°C until use.

2.5. Sample derivatization

Two-stage chemical derivatization (Li et al., 2012) was performed after drying the samples in a vacuum drying oven at 30°C for 24 h. The samples were dissolved in 100 μL of methoxyamine hydrochloride (20 mg/mL in pyridine) prior to incubation at 30°C for 2 h. One hundred microliters of N-methyl-N-(trimethylsilyl) trifluoroacetamide (MSTFA) was added to the samples before incubation at 30°C for 3 h to trimethylsilylate the polar functional groups. The derivate samples were rapidly filtered through 0.22-μm-diameter round hydrophobic nylon filters before GC-MS analysis.

2.6. GC-MS analysis

Chromatography analysis was performed on a QP2010 GC-MS system (Shimadzu Co., Japan) equipped with a DB-5 capillary column (30 m×250 mm id, 0.25 μm film thickness; Agilent J&W Scientific, Folsom, CA) with 70 eV of electron impact ionization. Derivatized samples (1 μL) were injected in split mode with a split ratio of 30:1 and injector temperature was set as 300°C. Helium was used as the carrier gas at a constant flow rate of 1 mL/min. The GC oven temperature program was initially set at 80°C for 1 min, then raised to 100°C at a rate of 2°C/min, and ramped to a final temperature of 300°C at a rate of 2°C/min and maintained at 300°C for 6min. The temperatures of ion source and ion source surface were set as 200°C and 280°C, respectively. Mass spectra were recorded by full scan mode in the mass range of 80-500 m/z at a rate of 20 scans/sec. Ribitol was used as an internal standard to monitor batch reproducibility and

correct for minor variations that occurred during sample preparation and analysis.

2.7. Data analysis and pattern recognition analysis

GC-MS Real Time Analysis software (Shimadzu Co., Japan) was used for processing the GC-MS data. Metabolites were identified by matching the data with the NIST mass spectral library (http://www.nist.gov/srd/). After being normalized against the internal standard (peak areas of ribitol) and dry weight of cells to acquire the relative abundance of metabolites, all the peak areas of identified metabolites were used as metabolomics profile data and then subjected to the software of SIMCA package 10.0 (Umetrics, Umea, Sweden).

After mean-centering and Par-scaling, the data were used for further analysis. Supervised partial least squares-discriminant analysis (PLS-DA) was initially performed to obtain an overview of the GC-MS data from different groups. To identify the butanol stress-associated metabolite changes during acidogenic and solventogenic phases, a PLS-DA pairwise comparison was subsequently carried out. Variables responsible for distinguishing butanol-treated groups from the control group (without butanol) were selected by loadings plots and variable importance in the projection (VIP) value threshold (VIP>1) from the 7-fold cross-validated PLS-DA models. Accuracy and predictive ability of the models were evaluated by R^2 and Q^2 values.

The identified differential metabolites elicited by butanol that were selected by the PLS-DA models were analyzed by another multivariate statistical analysis method, hierarchical cluster analysis (HCA), to assess the predictive accuracy of the PLS-DA models. HCA was performed with the aid of Cluster 3.0, and visualized using TreeView 1.1.6 software.

2.8. Statistical analysis

Independent-samples T test was performed on specific metabolites by IBM SPSS Statistics 20.0 (SPSS Inc., USA) to assess the statistical significance of the metabolic changes. Differences showing *P*-values less than 0.05 were considered statistically significant.

3. Results

3.1. Effect of butanol stress on the growth of C. acetobutylicum

The addition of butanol inhibited *C. acetobutylicum* cell growth, and the inhibitory degree increased as butanol concentration increased (Fig. 1). Compared with that of the control cells that did not receive butanol challenge, *C. acetobutylicum* biomass decreased about 22.6%, 23.4%, 56.2%, 93.1% and 95.1% under 0.5%, 1.0%, 1.5%, 2.0% and 2.5% v/v butanol stress, respectively, at 8 h (i.e., exponential phase), while decreased about 18.6%, 20.2%, 69.7%, 80.8% and 97.9% under 0.5%, 1.0%, 1.5%, 2.0% and 2.5% v/v butanol stress, respectively, at 24 h (i.e., stationary phases). *C. acetobutylicum* almost did not grow under high levels of butanol stress (i.e., 2.0% and 2.5% v/v) (Fig. 1), which was consistent with what reported by Knoshaug and his colleagues (Knoshaug and Zhang, 2009).

Fig. 1

3.2. Effect of butanol treatment on the intracellular metabolite profiles of C. acetobutylicum

For metabolomics analysis, *C. acetobutylicum* cells were harvested after 8 h (i.e.,

acidogenesis phase) and 24 h (i.e., solventogenesis phase) of incubation, respectively. Typical GC-MS total ion chromatogram (TIC) from the acidogenesis phase's and solventogenesis phase's *C. acetobutylicum* cells treated with various concentrations of butanol were respectively shown in Supplementary Figs. S1 and S2. About 150 peaks were detected and 135 compounds were identified as metabolites and used for subsequent metabolomics analysis. The PLS-DA 3D scatter plot with excellent fit and satisfactory predictive ability (Table 1) was performed to represent the overview of acidogenic and solventogenic phases sample distribution in the new multivariate space (Fig. 2A). The biological replicates of control group (without butanol addition) and butanol-treated groups were distinctly clustered in the plot; meanwhile the samples under intermediate (i.e., 1.5% v/v) and high (i.e., 2.0% and 2.5% v/v) concentration of butanol stress from different time points (acidogenic and solventogenic phases, i.e., 8 and 24 h) were separated as two parts (blue circle referred to 8 h and red circle referred to 24 h, respectively in Fig. 2A), suggesting that fermentation time make more contribution to the metabolic changes of *C. acetobutylicum* than butanol stress. Specially, distinct separation was observed among intermediate (i.e., 1.5% v/v) and high (i.e., 2.0% and 2.5% v/v) concentration of butanol treated groups across the time courses, while separations of the control and low butanol-treated groups (0.5% and 1.0% v/v) across the time courses were less obvious. In addition, a clear butanol concentration-dependent metabolic profile changing trajectory can be observed along PC1 (Fig. 2). A clear discrimination among low (0.5% and 1.0% v/v), intermediate (1.5% v/v) and high (2.0% and 2.5% v/v) concentration of butanol challenged groups was present (three green circles in Fig. 2A). To further confirm this pattern, an additional PLS-DA analysis of *C. acetobutylicum* metabolic profiles at each time point (i.e., 8 h and 24 h) was performed and results also showed a clear separation among low (0.5%

and 1.0% v/v), intermediate (1.5% v/v) and high (2.0% and 2.5% v/v) concentration of butanol-treated groups (Fig. 2B and 2C).

Fig. 2

Table 1

3.3. Changes of intracellular metabolites at each butanol concentration

The PLS-DA pairwise comparisons between the control group and each butanol-treated group at both acidogenic and solventogenic phases were performed and results suggested an distinct metabolic difference between the groups in each pairwise comparison on the first component (Fig. 3A, C, E, G and I for acidogenic phase; Fig. 4A, C, E, G and I for solventogenic phase). The PLS-DA models were well constructed with excellent fit and satisfactory predictive ability (Table 1). The major metabolic perturbations that cause above discriminations were identified from the line plots of the *X*-loadings of the first component of the PLS-DA models (Fig. 3B, D, F, H and J for acidogenic phase; Fig. 4B, D, F, H and J for solventogenic phase). The intensity of the peak presented contribution to the class separation. The VIP plots showed the order of identified metabolites contributed to the class separation (Supplementary Fig. S3 for acidogenic phase; Supplementary Fig. S4 for solventogenic phase). On the basis of *X*-loadings line plots and VIP plots, a total of 27 paired retention time-mass to charge ratio (RT-M/Z) variables contributing to the separation of the control group and butanol-treated groups at acidogenic and solventogenic phases were selected according to the cutoff VIP value (VIP>1) (Tables 2 and 3). The metabolites which were probably responsible for the butanol stress-associated intracellular

metabolic perturbations mainly included glycolysis and TCA cycle intermediates, saccharides, amino acids and fatty acids.

Fig. 3

Fig. 4

Table 2

Table 3

The HCA plot of the 27 identified differential metabolites reflected a clustering pattern that was similar to the PLS-DA analysis results at both acidogenic and solventogenic phases (Fig. 5). The intermediate (i.e., 1.5% v/v) and high (i.e., 2.0% and 2.5% v/v) concentration of butanol treated groups were separate from the control and low concentration (0.5% and 1.0% v/v) of butanol-treated groups (Fig. 5). The HCA result was consistent with the PLS-DA models, which also verified the predictive accuracy of the PLS-DA models.

Fig. 5

4. Discussion

In the biobutanol fermentation process, *C. acetobutylicum* is often stressed by different environmental factors, especially toxicity of the accumulated butanol (Tomas et al., 2004; Alsaker et al., 2010; Ghiaci et al., 2013; Nicolaou et al., 2010; Dash et al., 2014). The results presented here also confirmed the inhibition effect of butanol on the *C. acetobutylicum* growth, and the inhibitory effect presented a dose-dependent mode (Fig. 1). Moreover, the lag phase of butanol-treated groups was delayed (Fig. 1), suggesting that the cell cycle of *C. acetobutylicum* was prolonged under butanol stress. The decreased biomass and prolonged cell cycle were results of

interaction of many changed factors, molecules or reactions secondary to butanol stress. Metabolomics analysis, which assesses the last step of the series of changes, can directly reveal biological phenotypic changes and provide a powerful platform for revealing the exact mechanism underlying response or adaptation of *C. acetobutylicum* to butanol stress. In fact, compared with the control group that did not receive butanol challenge, butanol treatment did induce many metabolic changes at either exponential phase (i.e., acidogenesis) or stationary phase (i.e., solventogenesis), especially in the metabolisms of carbohydrates, lipids and amino acids.

Compared with the control group (without butanol), butanol stress promoted the intracellular accumulation of glucose and galactopyranose ($P<0.001$) at both middle exponential and early stationary phases (Tables 2 and 3, Fig. S5), indicating that glycolysis might be inhibited by butanol and the utilization of carbon sources for fermentation might be diminished. This might account for the inhibition of *C. acetobutylicum* growth by butanol stress (Fig. 1). Furthermore, butanol stress caused increase in the levels of valine, leucine, isoleucine, alanine, glycine, threonine, phenylalanine, tyrosine, tryptophan, glycerol, glycerol-3-phosphate and lactate at both middle exponential phase and stationary phase (Tables 2 and 3, Supplementary Fig. S5). These metabolites could be converted from dihydroxyacetone phosphate (DHAP) and pyruvate, which are both metabolic intermediates of the Embden–Meyerhof–Parnas (EMP) pathway (Supplementary Fig. S5). As seen from another perspective, to some extent, the levels of the metabolic intermediates of EMP pathway might decrease under butanol stress. The results also indicated that butanol stress might inhibit glycolysis of *C. acetobutylicum*. In consistent with our results, results reported by Tomas and his colleagues also revealed that glucose metabolism was negatively affected by butanol stress, and expressions of several glycolytic genes including 6-

phosphofructokinase (*pfkA*), glucose 6-phosphate isomerase (*pgi*), and pyruvate kinase (*pykA*) genes decreased in the butanol-challenged (0.25% and 0.75% v/v) cultures of *C. acetobutylicum* strain 824 (pGROE1) and the plasmid control strain 824 (pSOS95del) (Tomas et al., 2004). Another previous study also indicated that under butanol stress, expressions of glycolytic genes including glucokinase (*glcK*), phosphoglycerate mutase (*pgm*) and enolase (*eno*) were down-regulated (Alsaker et al., 2010). Moreover, under butanol stress, activated bioconversion of pyruvate to lactate and DHAP to glycerol-3-phosphate would consume more NADH, and higher glycerol production also consumed more NADH; on the other hand, activated TCA cycle produced more NADH (Figs. 5 and 6). These results suggested that the redox balance in *C. acetobutylicum* might be also disturbed by butanol stress (Fig. 6B).

Fig. 6

Butanol stress also induced the accumulation of glycerol at both middle exponential and early stationary phases ($P<0.001$) (Tables 2 and 3, Supplementary Fig. S5). Intracellular glycerol is considered as an important cytoprotectant (Tulha et al. 2010) and plays a vital role in the osmoadaptation of *S. cerevisiae* (Petelenz-Kurdziel et al. 2013). Similarly, increased glycerol in the butanol-treated groups might also confer butanol tolerance to *C. acetobutylicum*. It has been demonstrated that expressions of two glycerol metabolism genes, glycerol uptake facilitator (*glpF*) and glycerol-3-phosphate dehydrogenase (*glpA*), were up-regulated in *C. acetobutylicum* following the butanol stress challenge (Alsaker et al., 2010). In addition, the glycerol could accumulate at the expense of the biomass production, and hyperosmotic stress further induced redirecting of glycolytic flux from biomass production to glycerol accumulation (Petelenz-Kurdziel et al. 2013). In this work, increased glycerol secondary to butanol stress might also

indicate that glycolytic flux reroute from biomass towards production of glycerol accordingly with the inhibition of *C. acetobutylicum* cell growth (Fig. 6).

TCA cycle could provide many metabolic intermediates for the metabolism of certain amino acids, fatty acids and one-carbon compounds. It has been previously reported that *C. acetobutylicum* has a bifurcated TCA cycle; that is to say that oxaloacetate can flow to succinate through either malate/fumarate (reductive branch) or citrate/α-ketoglutarate (oxidative branch) (Amador-Noguez et al., 2010; Crown et al., 2011). Amador-Noguez and his colleagues suggested that such a bifurcated TCA cycle could play a role in cellular redox balance and succinate is a biosynthetic rate-limiting metabolite (Amador-Noguez et al., 2010). Compared with control group (without butanol addition), butanol-treated groups had higher succinate content (P<0.001) at both middle exponential and early stationary phases (Tables 2 and 3). This result suggested that butanol stress might facilitate TCA cycle of *C. acetobutylicum* at both middle exponential and early stationary phases (Fig. 6).

Compared with the control group without butanol stress, *C. acetobutylicum* cells treated with butanol challenge had higher levels of hexadecanoic acid, octadecanoic acid and monostearin at both middle exponential and early stationary phases (Tables 2 and 3, Supplementary Fig. S5). Total lipids of *C. acetobutylicum* have been indicated to account for 5-6% of the dry cell weight (Lepage et al., 1987). It has been also reported that butanol stress could lead to an increase of the ratio of saturated fatty acids to unsaturated membrane fatty acids (Baer et al., 1987), and changes of the mean fatty acid acyl chain length and changes of the membrane phospholipid composition (Lepage et al., 1987; Senger and Papoutsakis, 2008). Under butanol stress, the increased levels of saturated fatty acid and longer acyl chain fatty acids at the expense of unsaturated chains and

shorter acyl chains might confer butanol tolerance to *C. acetobutylicum* and counteract an increase of membrane fluidity induced by butanol (Baer et al., 1987, 1989; LePage et al., 1987; Schaffer et al., 2002). Our previous study also demonstrated that under ethanol stress, levels of long-chain saturated fatty acids (hexadecanoic and octadecanoic acids) increased significantly in *S. cerevisiae* (Li et al., 2012). More saturated and long-chain fatty acids might be the self-protection of *S. cerevisiae* to maintain the membrane integrity through decreasing membrane fluidity (Li et al., 2012). To some extent, increased hexadecanoic acid, octadecanoic acid and monostearin secondary to butanol stress might also play self-protective role in adaptation or tolerance of *C. acetobutylicum* to butanol response, even though the exact changes of plasma membrane under butanol stress remain unclear (Fig. 6).

The levels of amino acids (i.e., valine, leucine, isoleucine, threonine, glycine, alanine, phenylalanine, tyrosine, tryptophan, aspartate, glutamate, 5-oxo-proline and homocysteine) increased under butanol stress at both middle exponential and early stationary phases (Tables 2 and 3, Supplementary Fig. S5). The result suggested that *C. acetobutylicum* might adapt to butanol stress by regulating certain amino acids metabolism. Similar changes of valine, leucine, isoleucine and glutamine in *C. acetobutylicum* cells treated with 70 mM butanol or during the acidogenesis-solventogenic transition were detected (Amador-Noguez et al., 2011). Valine, leucine, and isoleucine are called branched-chain amino acids (BCAAs). Membrane fluidity changes of *Bacillus subtilis* can be accomplished by the synthesis of BCAAs (Mansilla et al., 2004). *C. acetobutylicum* might also adjust membrane fluidity with the increase of BCAAs in response to butanol stress. Expressions of BCAAs biosynthetic genes in *C. acetobutylicum* were up-regulated during the acidogenesis-solventogenic transition (Jones et al., 2008) or under butanol stress

(Alsaker et al., 2010). Moreover, supplementation with some amino acids will promote ethanol tolerance of yeast cells by stabilizing membrane structures (Ding et al., 2009). Gonzalez and his colleagues suggested that ethanol tolerance might concern with the increased metabolism of glycine and the addition of glycine increased ethanol tolerance in the parental KO11 strain (Gonzalez et al., 2003). Increased levels of these amino acids together with the other increased amino acids might also confer butanol tolerance to *C. acetobutylicum* (Fig. 6).

In summary, this work illustrated the utility of a GC-MS-based metabolomics strategy to evaluate the response or adaptation of *C. acetobutylicum* to butanol stress at middle exponential and early stationary phases. The quantitative metabolic profiling could effectively reveal group classification and clear pairwise discrimination between control (without butanol) and butanol-treated groups. The widespread changes in metabolite concentrations at both middle exponential and early stationary phases suggested that core metabolic fluxes of *C. acetobutylicum* might be affected by butanol stress; on the other hand, *C. acetobutylicum* cells might also remodel their metabolisms to acquire higher butanol tolerance. Under butanol stress, glycolysis might be inhibited and TCA might be promoted. In addition, changes of lipids and fatty acids composition, amino acid metabolism and osmoregulator concentrations might be the key protection factors against butanol stress. Results described here would highlight the understanding of the molecular mechanism of the response or adaptation of *C. acetobutylicum* to butanol stress. Fully understanding of this mechanism will facilitate the development of metabolic regulations to improve the butanol tolerance of *C. acetobutylicum* and contribute to the construction of feasible butanologenic strains with higher butanol tolerance for better fermentative capacities.

Acknowledgements

This work was partially supported by the Strategic Priority Research Program of the Chinese Academy of Sciences (No. XDB14010301) and the Fundamental Research Funds for the Central Universities (No. YS1407).

Appendix A. Supplementary data

Supplementary data associated with this article can be found in the online version.

References

Alsaker KV, Spitzer TR, Papoutsakis ET. Transcriptional analysis of spo0A overexpression in *Clostridium acetobutylicum* and its effect on the cell's response to butanol stress. J Bacteriol 2004; 186: 1959-71.

Alsaker KV, Paredes C, Papoutsakis ET. Metabolite stress and tolerance in the production of biofuels and chemicals: Gene-expression-based systems analysis of butanol, butyrate, and acetate stresses in the anaerobe *Clostridium acetobutylicum*. Biotechnol Bioeng 2010; 105: 1131-47.

Amador-Noguez D, Feng XJ, Fan J, Roquet N, Rabitz H, Rabinowitz JD. Systems-level metabolic flux profiling elucidates a complete, bifurcated tricarboxylic acid cycle in *Clostridium acetobutylicum*. J Bacteriol 2010; 192: 4452-61.

Amador-Noguez D, Brasg IA, Feng XJ, Roquet N, Rabinowitz JD. Metabolome remodeling during the acidogenic-solventogenic transition in *Clostridium acetobutylicum*. Appl Environ

Microbiol 2011; 77: 7984-97.

Baer SH, Blaschk HP, Smith TL. Effect of butanol challenge and temperature on lipid composition and membrane fluidity of butanol-tolerant *Clostridium acetobutylicum*. Appl Environ Microbiol 1987; 53: 2854-61.

Baer SH, Bryant DL, Blaschek HP. Electron spin resonance analysis of the effect of butanol on the membrane fluidity of intact cells of *Clostridium acetobutylicum*. Appl Environ Microbiol 1989; 55: 2729-31.

Crown SB, Indurthi DC, Ahn WS, Choi J, Papoutsakis ET, Antoniewicz MR. Resolving the TCA cycle and pentose-phosphate pathway of *Clostridium acetobutylicum* ATCC 824: isotopomer analysis, in vitro activities and expression analysis. Biotechnol J 2011; 6: 300-5.

Cui FX, Zhang RM, Liu HQ, Wang YF, Li H. Metabolic responses to *Lactobacillus plantarum* contamination or bacteriophage treatment in *Saccharomyces cerevisiae* using a GC-MS-based metabolomics approach. World J Microbiol Biotechnol 2015; 31: 2003-13.

Dash S, Mueller TJ, Venkataramanan KP, Papoutsakis ET, Maranas CD. Capturing the response of *Clostridium acetobutylicum* to chemical stressors using a regulated genome-scale metabolic model. Biotechnol Biofuels 2014; 7: 144.

Ding JM, Huang XW, Zhang LM, Zhao N, Yang DM, Zhang KQ. Tolerance and stress response to ethanol in the yeast *Saccharomyces cerevisiae*. Appl Microbiol Biotechnol 2009; 85: 253-63.

Dürre P. Biobutanol: an attractive biofuel. Biotechnol J 2007; 2: 1525-34.

Ghiaci P, Norbeck J, Larsson C. Physiological adaptations of *Saccharomyces cerevisiae* evolved for improved butanol tolerance. Biotechnol Biofuels 2013; 6: 101.

Gonzalez R, Tao H, Purvis JE, York SW, Shanmugam KT, Ingram LO. Gene array-based

identification of changes that contribute to ethanol tolerance in ethanologenic *Escherichia coli*: comparison of KO11 (parent) to LY01 (resistant mutant). Biotechnol Prog 2003; 19: 612-23.

Green EM. Fermentative production of butanol-the industrial perspective. Curr Opin Biotechnol 2011; 22: 337-43.

Gu Y, Jiang Y, Wu H, Liu X, Li Z, Li J, Xiao H, Shen Z, Dong H, Yang Y, Li Y, Jiang W, Yang S. Economical challenges to microbial producers of butanol: feedstock, butanol ratio and tite. Biotechnol J 2011; 6: 1348-57.

Hillmann F, Fischer RJ, Saint-Prix F, Girbal L, Bahl H. PerR acts as a switch for oxygen tolerance in the strict anaerobe *Clostridium acetobutylicum*. Mol Microbiol 2008; 68: 848-60.

Hu X, Li H, Tang P, Sun J, Yuan Q, Li C. GC-MS-based metabolomics study of the responses to arachidonic acid in *Blakeslea trispora*. Fungal Genet Biol 2013; 57: 33-41.

Jang YS, Han MJ, Lee J, Im JA, Lee YH, Papoutsakis ET, Bennett G, Lee SY. Proteomic analyses of the phase transition from acidogenesis to solventogenesis using solventogenic and non-solventogenic *Clostridium acetobutylicum* strains. Appl Microbiol Biotechnol 2014; 98: 5105-15.

Jones SW, Paredes CJ, Tracy B, Cheng N, Sillers R, Senger RS, Papoutsakis ET. The transcriptional program underlying the physiology of clostridial sporulation. Genome Biol 2008; 9: R114.

Knoshaug EP, Zhang M. Butanol tolerance in a selection of microorganisms. Appl Biochem Biotechnol 2009; 153: 13-20.

Ku KM, Kim J, Park HJ, Liu KH, Lee CH. Application of metabolomics in the analysis of

manufacturing type of pu-erh tea and composition changes with different postfermentation year. J Agric Food Chem 2010; 58: 345-52.

Kumar M, Gayen K. Developments in biobutanol production: new insights. Appl Energ 2011; 88: 1999-2012.

Lee SH, Kim S, Kwon MA, Jung YH, Shin YA, Kim KH. Atmospheric vs. anaerobic processing of metabolome samples for the metabolite profiling of a strict anaerobic bacterium, *Clostridium acetobutylicum*. Biotechnol Bioeng 2014; 111: 2528-36.

LePage C, Fayolle F, Hermann M, Vandecasteele JP; Changes in membrane lipid composition of *Clostridium acetobutylicum* during acetone butanol fermentation: effects of solvents, growth temperature and pH. J Gen Microbiol 1987; 133: 103-10.

Liao C, Seo SO, Celik V, Liu H, Kong W, Wang Y, Blaschek H, Jin YS, Lu T. Integrated, systems metabolic picture of acetone-butanol-ethanol fermentation by *Clostridium acetobutylicum*. Proc Natl Acad Sci USA 2015; 112 (27): 8505-10.

Li H, Ma ML, Luo S, Zhang RM, Han P, Hu W. Metabolic responses to ethanol in *Saccharomyces cerevisiae* using a gas chromatography tandem mass spectrometry-based metabolomics approach. Int J Biochem Cell Biol 2012; 44: 1087-96.

Lütke-Eversloh T, Bahl H. Metabolic engineering of *Clostridium acetobutylicum*: recent advances to improve butanol production. Curr Opin Biotechnol 2011; 22 (5): 634-47.

Mansilla MC, Cybulski LE, Albanesi D, de Mendoza D. Control of membrane lipid fluidity by molecular thermosensors. J Bacteriol 2004; 186: 6681-8.

Nicolaou SA, Gaida SM, Papoutsakis ET. A comparative view of metabolite and substrate stress and tolerance in microbial bioprocessing: From biofuels and chemicals, to biocatalysis and

bioremediation. Metab Eng 2010; 12: 307-31.

Nölling J, Breton G, Omelchenko MV, Makarova KS, Zeng Q, Gibson R, Lee HM, Dubois J, Qiu D, Hitti J, Wolf YI, Tatusov RL, Sabathe F, Doucette-Stamm L, Soucaille P, Daly MJ, Bennett GN, Koonin EV, Smith DR. Genome sequence and comparative analysis of the solvent-producing bacterium *Clostridium acetobutylicum*. J Bacteriol 2011; 183: 4823-38.

Petelenz-Kurdziel E, Kuehn C, Nordlander B, Klein D, Hong KK, Jacobson T, Dahl P, Schaber J, Nielsen J, Hohmann S, Klipp E. Quantitative analysis of glycerol accumulation, glycolysis and growth under hyper osmotic stress. PLoS Comput Biol 2013; 9: e1003084.

Schaffer S, Isci N, Zickner B, Dürre P. Changes in protein synthesis and identification of proteins specifically induced during solventogenesis in *Clostridium acetobutylicum*. Electrophoresis 2002; 23: 110-21.

Senger RS, Papoutsakis ET. Genome-scale model for *Clostridium acetobutylicum*: Part I. Metabolic network resolution and analysis. Biotechnol Bioeng 2008; 101: 1036-52.

Tomas CA, Welker NE, Papoutsakis ET. Overexpression of groESL in *Clostridium acetobutylicum* results in increased solvent production and tolerance, prolonged metabolism, and changes in the cell's transcriptional program. Appl Environ Microbiol 2003; 69: 4951-65.

Tomas CA, Beamish J, Papoutsaki ET. Transcriptional analysis of butanol stress and tolerance in *Clostridium acetobutylicum*. J Bacteriol 2004; 186: 2006-18.

Tulha J, Lima A, Lucas C, Ferreira C. *Saccharomyces cerevisiae* glycerol/H+ symporter Stl1p is essential for cold/near-freeze and freeze stress adaptation. A simple recipe with high biotechnological potential is given. Microb Cell Fact 2010; 9: 82.

Zhao Y, Hindorff LA, Chuang A, Monroe-Augustus M, Lyristis M, Harrison ML, Rudolph FB,

Bennett GN. Expression of a cloned cyclopropane fatty acid synthase gene reduces solvent formation in *Clostridium acetobutylicum* ATCC 824. Appl Environ Microbiol 2003; 69: 2831-41.

Zheng YN, Li LZ, Xian M, Ma YJ, Yang JM, Xu X, He DZ. Problems with the microbial production of butanol. J Ind Microbiol Biotechnol 2009; 36: 1127-38.

Figure Legends

Fig. 1. Effect of different concentrations of butanol on the growth of *C. acetobutylicum.* **P*<0.05 compared to the control group (without butanol); ***P*<0.01 compared to the control group (without butanol).

Fig. 2. PLS-DA-derived scores plots for control group without butanol and butanol treated groups at (A) both middle exponential phase and stationary phase, (B) middle exponential phase, and (C) stationary phase. Blue shadow arrow and pink shadow arrow respectively represent the butanol concentration-dependent moving trajectory at the middle exponential phase and the stationary phase. The clustering patterns of different fermentation time points are indicated by blue circle at middle exponential phase and red circle at stationary phase, respectively. The clustering patterns of different butanol concentrations are indicated by green circle. In the scores plot, the confidence interval is defined by the Hotelling's T2 ellipse (95% confidence interval), and observations outside the confidence ellipse are considered outliers.

Fig. 3. PLS-DA model plots for the control group without butanol (gray symbols) versus group treated with different concentrations of butanol (red symbols) at acidogenic phase. Cross-validated scores plots of the pairwise comparison between the (A) control versus 0.5%, (C) control versus 1.0%, (E) control versus 1.5%, (G) control versus 2.0%, and (I) control versus 2.5% v/v butanol treated groups. Two groups in each scores plot were separated along the first component. In the scores plots, the confidence interval is defined by the Hotelling's T2 ellipse (95% confidence interval), and observations outside the confidence ellipse are considered outliers. Loading plots of pairwise comparison between (B) control versus 0.5%, (D) control versus 1.0%,

(F) control versus 1.5%, (H) control versus 2.0%, and (J) control versus 2.5% v/v butanol treated groups. The metabolites with the largest intensities contributed to the clustering.

Fig. 4. PLS-DA model plots for the control group without butanol (gray symbols) versus group treated with different concentrations of butanol (red symbols) at solventogenic phase. Cross-validated scores plots of the pairwise comparison between the (A) control versus 0.5%, (C) control versus 1.0%, (E) control versus 1.5%, (G) control versus 2.0%, and (I) control versus 2.5% v/v butanol treated groups. Two groups in each scores plot were separated along the first component. In the scores plots, the confidence interval is defined by the Hotelling's T2 ellipse (95% confidence interval), and observations outside the confidence ellipse are considered outliers. Loading plots of pairwise comparison between (B) control versus 0.5%, (D) control versus 1.0%, (F) control versus 1.5%, (H) control versus 2.0%, and (J) control versus 2.5% v/v butanol treated groups. The metabolites with the largest intensities contributed to the clustering.

Fig. 5. Hierarchical cluster analysis of the 27 identified differential metabolites at (A) middle exponential phase, and (B) stationary phase.

Fig. 6. Overview of the effect of butanol stress on (A) metabolic changes in *C. acetobutylicum* during acidogenic and solventogenic phases and (B) remodeling of *C. acetobutylicum* metabolism for acquiring higher of butanol tolerance. Solid blue circles represent butanol molecules. Red diamonds indicate positive regulation and green bars indicate negative regulation. The 'traffic light' denotes the control switch of metabolic regulation. Red symbol denotes turning up the switch and green symbol denotes turning down the switch, whereas yellow symbol denotes the balance of the switch.

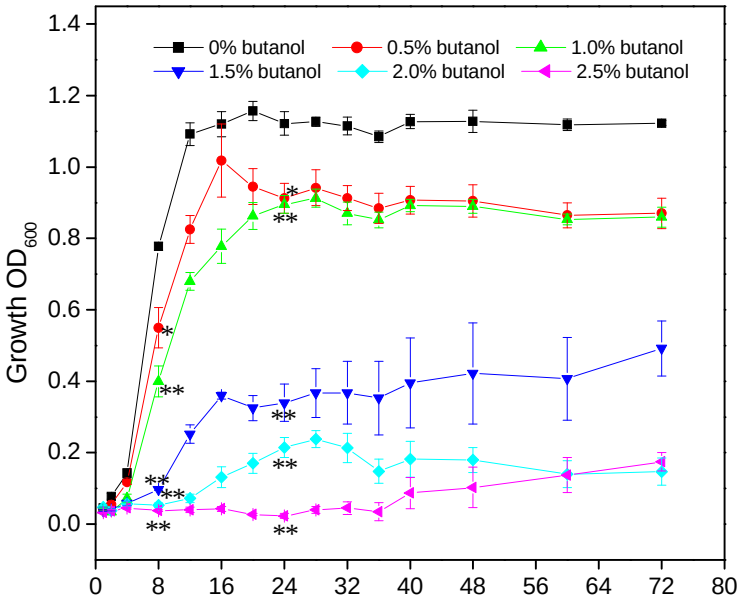

Fig. 1

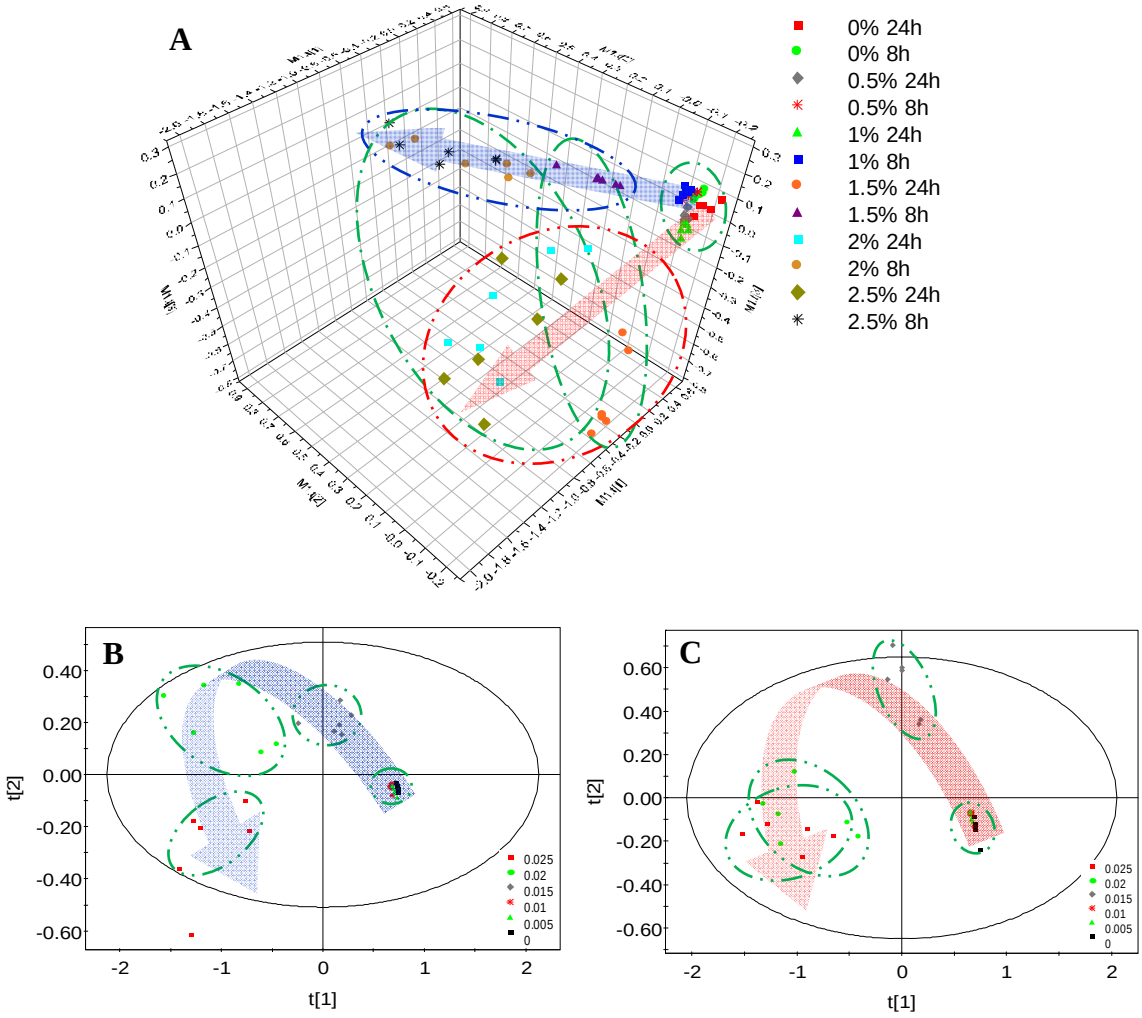

Fig. 2

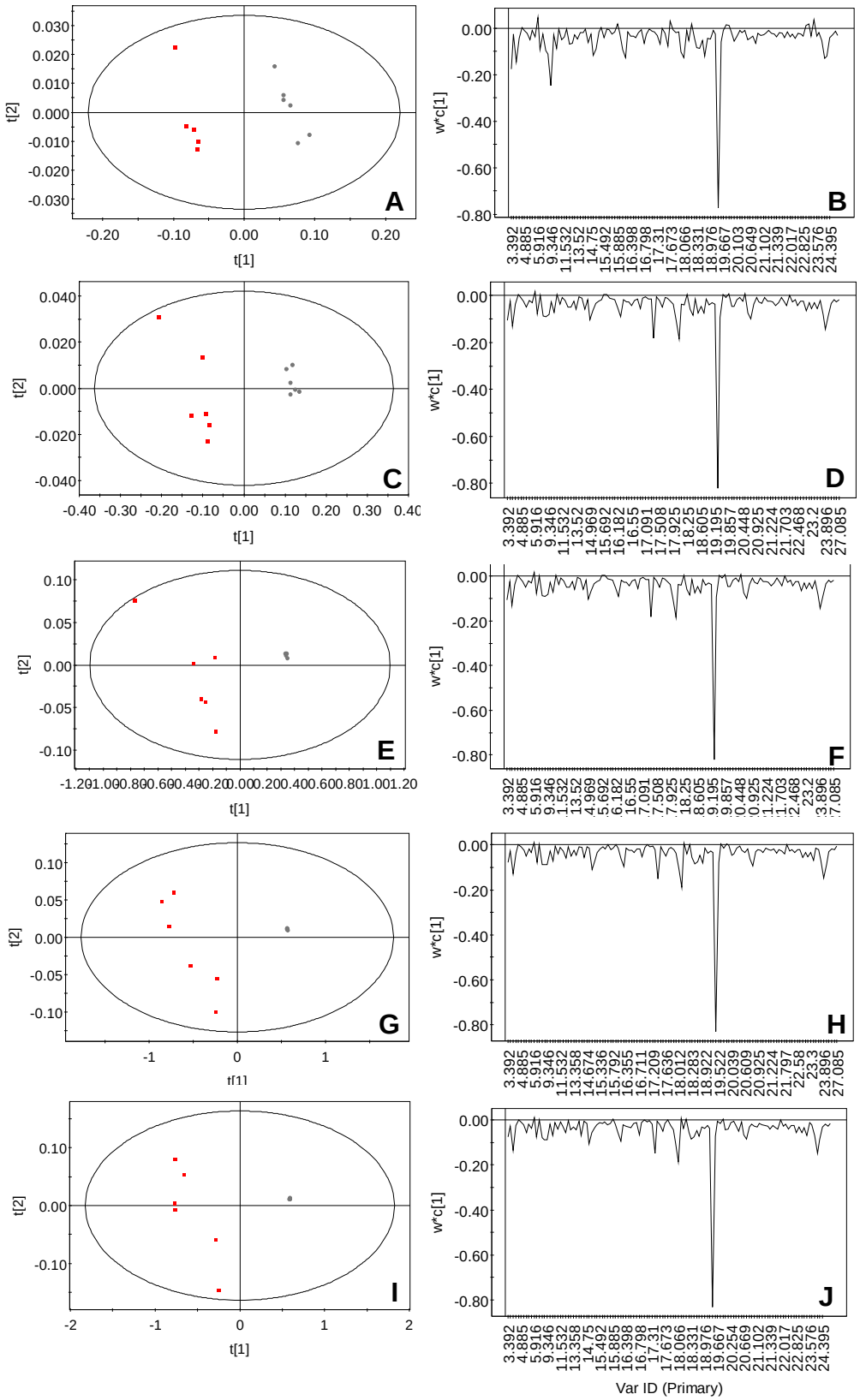

Fig. 3

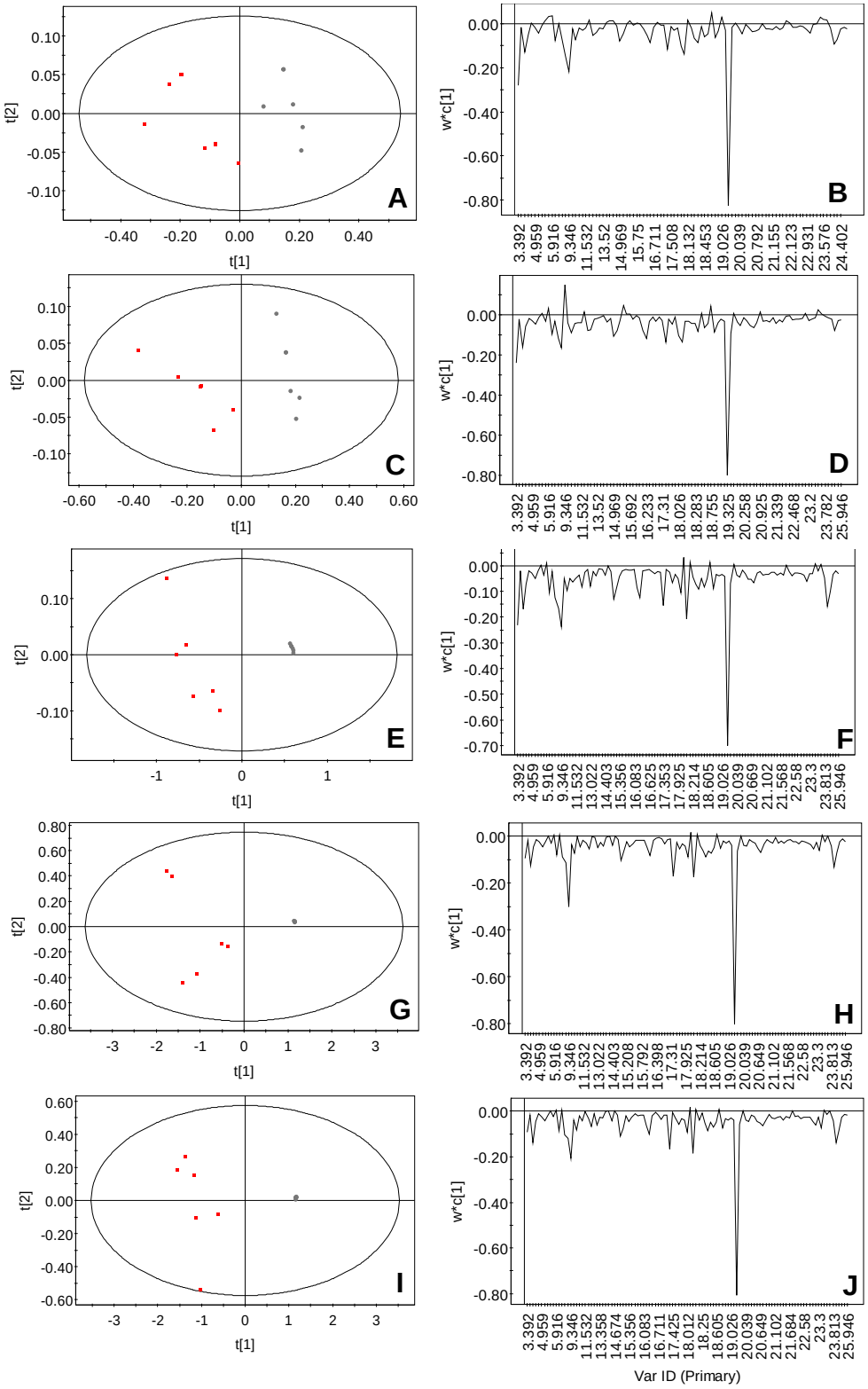

Fig. 4

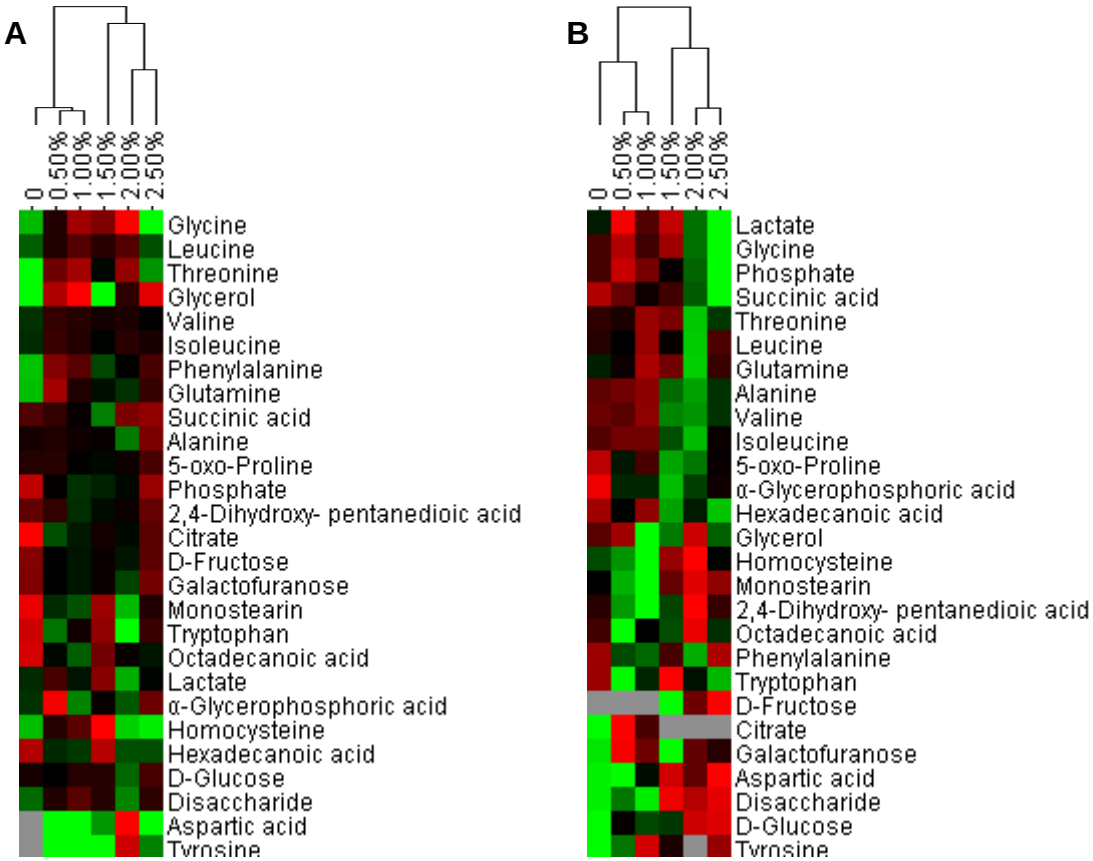

Fig. 5

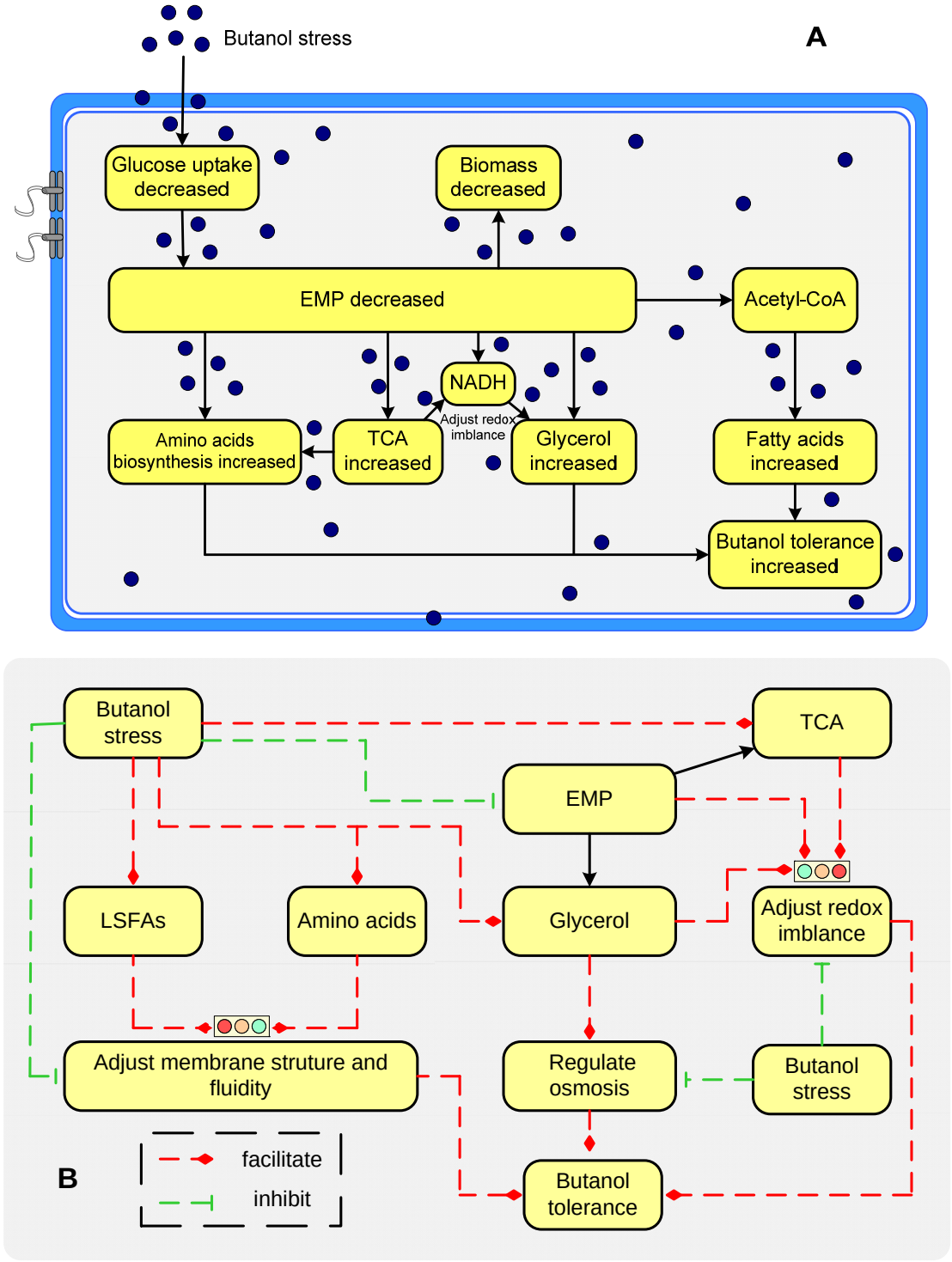

Fig. 6

Table 1

Statistical data from partial least squares-discriminant analysis (PLS-DA) models at different concentrations of butanol.

Sample	PLS PC'S	R^2X(cum)	R^2Y(cum)	Q^2(cum)
All	10	0.852	0.716	0.581
8-h treatment	7	0.862	0.853	0.67
24-h treatment	7	0.88	0.895	0.784
8-h 0% versus 0.5%	2	0.927	0.992	0.97
8-h 0% versus 1.0%	3	0.983	0.995	0.95
8-h 0% versus 1.5%	3	0.992	0.995	0.923
8-h 0% versus 2.0%	2	0.979	0.986	0.938
8-h 0% versus 2.5%	2	0.981	0.98	0.959
24-h 0% versus 0.5%	4	0.97	0.984	0.875
24-h 0% versus 1.0%	3	0.947	0.986	0.884
24-h 0% versus 1.5%	3	0.986	0.997	0.966
24-h 0% versus 2.0%	2	0.975	0.923	0.885
24-h 0% versus 2.5%	2	0.99	0.977	0.962

Table 2

The intracellular metabolites of *C. acetobutylicum* identified by GC-MS that differ between the control group (without butanol) and the butanol-treated groups at middle exponential phase (8h).

RT	Metabolite	Butanol content(v/v)					
		0%	0.5%	1.0%	1.5%	2.0%	2.5%
3.392	Lactate	0.1170±0.0060	0.1616±0.0024***	0.1940±0.0362***	0.4688±0.0579***	0.6430±0.0466***	0.6473±0.0364***
4.075	Alanine	0.0310±0.0014	0.0587±0.0008***	0.0990±0.0063***	0.5645±0.0677***	1.5181±0.1659***	1.6860±0.1314***
4.404	Glycine	0.0037±0.0004	0.0071±0.0008**	0.0128±0.0008***	0.0524±0.0104**	0.1476±0.0388*	0.0966±0.0357*
6.889	Valine	0.0109±0.0007	0.0221±0.0004***	0.0371±0.0020***	0.2009±0.0238***	0.5629±0.0667***	0.5150±0.0419***
8.911	Leucine	0.0123±0.0012	0.0250±0.0010***	0.0470±0.0027***	0.2450±0.0238***	0.7122±0.1017***	0.5789±0.0524***
9.133	Phosphate	0.0393±0.0008	0.0556±0.0013***	0.0777±0.0045***	0.3062±0.0443**	0.6933±0.0655***	0.7297±0.0456***
9.346	Glycerol	0.1249±0.0055	0.2065±0.0053***	0.3476±0.0260***	0.3321±0.0375***	0.7978±0.0375***	0.8402±0.0549***
9.723	Isoleucine	0.0100±0.0005	0.0201±0.0006***	0.0330±0.0019***	0.1700±0.0219***	0.4847±0.0561***	0.4507±0.0365***
10.530	Succinic acid	0.0055±0.0004	0.0090±0.0001***	0.0135±0.0010***	0.0505±0.0086**	0.1466±0.0155***	0.1462±0.0115***
13.022	Threonine	0.0037±0.0005	0.0096±0.0006***	0.0182±0.0010***	0.0747±0.0082***	0.2405±0.0395**	0.1768±0.0195***
13.520	Homocysteine	0.0021±0.0002	0.0054±0.0005***	0.0119±0.0019**	0.1159±0.0170***	0.2336±0.0648*	0.0123±0.0123***
14.969	5-oxo-Proline	0.0216±0.0007	0.0406±0.0015***	0.0652±0.0035***	0.3674±0.0533***	1.0476±0.1030***	1.0422±0.0793***
15.131	Aspartic acid	0.0018±0.0006	0.0127±0.0008***	0.0210±0.0012***	0.1353±0.0153***	0.4485±0.0628***	0.3214±0.0623**
16.182	Phenylalanine	0.0079±0.0010	0.0193±0.0012***	0.0313±0.0023***	0.1362±0.0226**	0.4095±0.0468***	0.4162±0.0483***
16.233	Glutamine	0.0116±0.0010	0.0331±0.0016***	0.0474±0.0026***	0.2774±0.0446**	0.8286±0.1014***	0.8407±0.0996***
17.636	Glycerophosphate	0.0047±0.0003	0.0126±0.0006***	0.0117±0.0007***	0.0849±0.0157***	0.2157±0.0268***	0.2306±0.0218***
18.012	D-Fructose	0.0229±0.0010	0.0373±0.0005***	0.0611±0.0036***	0.3654±0.0492***	0.9867±0.0867***	1.0186±0.0709***
18.066	Citrate	0.0713±0.0027	0.0937±0.0011***	0.1753±0.0105***	1.1310±0.1430***	3.1478±0.2960***	3.2056±0.2137***
18.331	Galactofuranose	0.0157±0.0008	0.0261±0.0007***	0.0432±0.0025***	0.2752±0.0392***	0.7541±0.0763***	0.8100±0.0513***
18.453	Dihydroxypentanedioic	0.0130±0.0007	0.0229±0.0004***	0.0331±0.0029***	0.1881±0.0303**	0.5128±0.0575***	0.5138±0.0264***
18.881	Tyrosine	0.0014±0.0014	0.0214±0.0008***	0.0326±0.0017***	0.1796±0.0337**	0.6235±0.0905***	0.5111±0.0793***
19.325	D-Glucose	0.8938±0.0503	1.6886±0.0402***	3.2651±0.1920***	21.9818±2.9785***	60.9150±6.1392***	65.2951±6.4176***
19.522	Hexadecanoic acid	0.0150±0.0013	0.0222±0.0027*	0.0350±0.0019***	0.2721±0.0263***	0.5432±0.0432***	0.4985±0.0300***
20.649	Tryptophan	0.0101±0.0007	0.0135±0.0020***	0.0270±0.0014***	0.1835±0.0188***	0.3636±0.0350***	0.4157±0.0385***
20.792	Octadecanoic acid	0.0169±0.0016	0.0264±0.0044	0.0371±0.0018***	0.3086±0.0251***	0.7545±0.0663***	0.6890±0.0354***
23.813	Monostearin	0.0104±0.0007	0.0149±0.0009**	0.0234±0.0011***	0.2056±0.0160***	0.4254±0.0274***	0.4576±0.0258***
23.896	Disaccharide	0.0317±0.0020	0.0766±0.0050***	0.1631±0.0075***	1.1599±0.1575***	3.4685±0.3977***	3.6079±0.1515***

Note. The VIP scores of all listed metabolites are greater than 1.

The data represents the relative peak intensity and are presented as the mean ± SEM.

*P<0.05 compared with the control; **P<0.01 compared with the control; ***P<0.001 compared with the control.

Table 3

The intracellular metabolites of *C. acetobutylicum* identified by GC-MS that differ between the control group (without butanol) and the butanol-treated groups at stationary phase (24h).

		Butanol content(v/v)					
RT	Metabolite	0%	0.5%	1.0%	1.5%	2.0%	2.5%
3.392	Lactate	0.2047±0.0440	0.6841±0.0733***	0.6575±0.0923***	4.5907±0.3731***	3.1173±0.4148***	2.9736±0.2807***
4.075	Alanine	0.1705±0.0204	0.2907±0.0299**	0.3623±0.0303***	2.4832±0.1751***	5.2137±0.5680***	6.3269±0.4723***
4.404	Glycine	0.0302±0.0056	0.0522±0.0066*	0.0580±0.0054**	0.4625±0.0402***	0.7443±0.1107***	0.8122±0.1542**
6.889	Valine	0.0671±0.0089	0.1106±0.0109	0.1395±0.0106***	0.9524±0.0703***	2.0463±0.1982***	2.4464±0.1645***
8.911	Leucine	0.0889±0.0146	0.1429±0.0147*	0.1926±0.0144***	1.3764±0.1072***	2.5931±0.3157***	3.5980±0.2687***
9.133	Phosphate	0.1632±0.0129	0.3048±0.0309**	0.3608±0.0303***	2.4148±0.1794***	5.3766±1.5179**	4.6679±0.3294***
9.346	Glycerol	0.7075±0.1123	1.1842±0.2150	0.4539±0.0307	5.7012±0.7539***	37.3572±10.5260*	15.7108±2.7027**
9.723	Isoleucine	0.0560±0.0073	0.0962±0.0104**	0.1164±0.0091***	0.8367±0.0556***	1.7264±0.2094***	2.1669±0.1428***
10.530	Succinic acid	0.0316±0.0042	0.0426±0.0049	0.0487±0.0050*	0.3699±0.0309***	0.6582±0.0903***	0.6166±0.0474***
13.022	Threonine	0.0379±0.0078	0.0556±0.0055	0.0837±0.0077**	0.5715±0.0519***	0.8108±0.1176***	1.2136±0.1285***
13.520	Homocysteine	0.0065±0.0001	0.0104±0.0012*	0.0102±0.0014*	0.1454±0.0173***	0.5316±0.0689***	0.3049±0.0307***
14.969	5-oxo-Proline	0.1105±0.0156	0.1645±0.0152*	0.2087±0.0194**	1.5117±0.1126***	3.4364±0.3723***	4.0270±0.3157***
15.131	Aspartic acid	0.0227±0.0034	0.0397±0.0043*	0.0676±0.0075***	0.6275±0.0521***	1.3867±0.1822***	1.8407±0.1793***
16.182	Phenylalanine	0.0570±0.0084	0.0818±0.0138	0.0925±0.0105*	0.8259±0.0750***	1.6709±0.3164**	2.2079±0.0995***
16.233	Glutamine	0.0783±0.0132	0.1343±0.0137*	0.1898±0.0202***	1.3730±0.1117***	2.3868±0.4009**	3.3558±0.3069***
17.636	Glycerophosphate	0.0358±0.0030	0.0456±0.0054	0.0553±0.0049**	0.3881±0.0323***	0.9291±0.0887***	1.1430±0.1225***
18.012	D-Fructose	0.0000	0.0000	0.0000	4.3505±0.3096***	12.0288±1.0995***	13.4479±0.8771***
18.066	Citrate	0.0869±0.0134	0.2201±0.0344**	0.2473±0.0435**	0***	0***	0***
18.331	Galactofuranose	0.0483±0.0031	0.1497±0.0185**	0.1680±0.0182***	0.8598±0.0745***	2.8716±0.2374***	2.9029±0.2522***
18.453	Dihydroxypentanedioic	0.0380±0.0039	0.0623±0.0057**	0.0692±0.0055***	0.6475±0.0859***	1.7678±0.2522***	1.6173±0.1258***
18.881	Tyrosine	0.0366±0.0059	0.0695±0.0109*	0.0921±0.0105***	0.6959±0.0611***	1.1383±0.3509*	1.8596±0.2548***
19.325	D-Glucose	1.3152±0.2070	5.2579±0.5385***	5.9258±0.6824***	41.2132±3.3527***	204.7982±20.7503***	206.2013±12.1761***
19.522	Hexadecanoic acid	0.0642±0.0045	0.0700±0.0054	0.1245±0.0081***	0.5410±0.1080**	1.3610±0.2056***	1.2041±0.1588***
20.649	Tryptophan	0.0259±0.0022	0.0366±0.0035*	0.0480±0.0033***	0.4897±0.1009**	0.9362±0.1449**	0.9105±0.0905***
20.792	Octadecanoic acid	0.0365±0.0050	0.0499±0.0071	0.0727±0.0084**	0.5710±0.0877**	1.6474±0.2484***	1.3937±0.1295***
23.813	Monostearin	0.0120±0.0012	0.0161±0.0010*	0.0153±0.0015	0.2074±0.0169***	0.6790±0.1395**	0.5762±0.0531***
23.896	Disaccharide	0.0325±0.0038	0.1140±0.0131***	0.0897±0.0120***	3.4998±0.3514***	9.9242±1.0514***	11.9427±1.1158***

Note. The VIP scores of all listed metabolites are greater than 1.

The data represents the relative peak intensity and are presented as the mean ± SEM.

*P<0.05 compared with the control; **P<0.01 compared with the control; ***P<0.001 compared with the control.